Experimental evidence of different hydrogen donors in *n*-type InN

G. Pettinari, F. Masia, M. Capizzi, and A. Polimeni
CNISM and Dipartimento di Fisica, Sapienza Università di Roma, Piazzale Aldo Moro 2, 00185 Roma, Italy

M. Losurdo and G. Bruno
Institute of Inorganic Methodologies and of Plasmas, IMIP-CNR, via Orabona 4, 70125 Bari, Italy

T. H. Kim, S. Choi, and A. Brown
Electrical and Computer Engineering Department, Duke University, Durham, North Carolina 27708, USA

V. Lebedev, V. Cimalla, and O. Ambacher
Fraunhofer Institute for Applied Solid State Physics, Tullastrasse 72, 79108 Freiburg, Germany
(Received 23 November 2007; revised manuscript received 14 January 2008; published 11 March 2008)

The multiform donor nature of hydrogen in *n*-type indium nitride is experimentally observed in samples exposed to atomic hydrogen. Photoluminescence measurements reveal a tenfold increase in the electron concentration and the formation of a shallow donor band upon hydrogen incorporation. Annealing studies show that hydrogen occupies at least two equilibrium sites having almost equivalent thermal stability.

DOI: 10.1103/PhysRevB.77.125207 PACS number(s): 71.55.Eq, 61.72.uj, 78.55.Cr

I. INTRODUCTION

Hydrogen behavior in semiconductors has been deeply investigated since Mollwo suggested[1] that H could be responsible for the resistivity increase observed upon H diffusion in ZnO and it was later realized that this ubiquitous, highly mobile, and reactive impurity passivates most deep and shallow defects purposely or accidentally present in many steps of semiconductor growth and device processing.

In the past few years, new surprising aspects of hydrogen behavior in semiconductors have been experimentally found and theoretically predicted. In dilute nitrides such as GaAsN and GaPN, and in II-O-VI compounds such as ZnTe:O hydrogen passivates, respectively, N and O, elements behaving as isoelectronic impurities in those alloys.[2–5] Moreover, hydrogen should act as a donor in *n*-type ZnO,[6] contrary to the amphoteric compensating behavior it shows in all other semiconductors. In particular, it was suggested that hydrogen displays a purely donor behavior whenever its pinning level resonates with the conduction band of the host material.[7,8] This is the case, indeed, of H in ZnO as well as in zinc blende InN,[9] two materials whose electron affinities are the highest among all semiconductors.

As regards InN, this compound has raised an increasing interest since 2002, when it has been found[10] that its energy gap is as low as 0.65 eV, namely, about one-fifth of that of its wide-gap parent compound, GaN. This small band gap energy is of great interest for photovoltaic applications of InN, since it would permit us to extend the absorption window of nitrides over the entire frequency region of the solar spectrum. Furthermore, the electron mobility of InN should be quite high, that renders this material very attractive for realizing high frequency electronic devices.[11]

However, good quality InN epitaxial layers have been obtained only very recently. Therefore, several aspects concerning the material's structural and defect properties are still debated,[10] in particular, doping, an issue of primary interest for any "new" material, and how to grow intrinsic InN. Moreover, whether Si impurities are donors or acceptors in InN has also been argument of debate[12] and only recently it has been claimed[13] that InN may be doped *p* type by Mg. As regards H, its donor nature has been inferred by muon spin resonance[14] and glow discharge and mass spectroscopy measurements[15] in wurtzite InN. Furthermore, a carrier concentration increase has been observed[16] in InN irradiated with high-energy (MeV) electrons. However, similar increases in carrier concentration observed upon bombardment with high energy (MeV) protons and $^4He^+$ particles[16] have been attributed to damage-induced point defects, in particular, to nitrogen vacancies.

This scenario highlights the manifold aspects that H plays in technologically relevant materials, such as ZnO and InN, and calls for a deeper comprehension of the electronic effects H creates therein.

In this paper, we report on a detailed analysis of photoluminescence (PL) spectra taken in state of the art wurtzite InN epitaxial layers, as grown or hydrogenated by a remote H_2 plasma or by a *low-energy* ion beam source. The electron concentration, in the range of 10^{17} cm^{-3} in the as-grown samples, increases gradually up to values of order of 10^{19} cm^{-3} upon incorporation of H atoms. A comparison with the effects produced by irradiation with $^4He^+$ particles rules out that this increase is due to mere damage-induced effects. Then, a detailed analysis of H thermal desorption from the samples has been performed at different annealing temperatures. It shows that hydrogen in *n*-type InN has two stable equilibrium donor sites, almost equivalent in energy, in agreement with suggestions based on first-principles calculations in zinc blende InN.[17] Finally, the shallow nature of H donors in InN is confirmed by the direct estimate of their binding energy, roughly 10 meV, which well agrees with the muon binding energy in this same material.[14]

II. EXPERIMENT

One set of 0.3 μm thick InN epilayers (D110 and D112) was grown by radio-frequency plasma-assisted molecular

beam epitaxy (MBE) on a Si-face 6H-SiC(0001) substrate.[18] X-ray diffraction (XRD) showed highly (0001)-oriented layers and different optical techniques[18] indicated no metallic indium inclusions. Another set of thicker ($\sim$0.9 μm) InN samples (IC205 and IO207) was also grown by MBE on different *in situ* prepared epitaxial templates [i.e., GaN(0001)/AlN/SiC/Si or GaN(0001)/AlN/Al_2O_3], as reported elsewhere.[19] Full width at half maximum of their rocking curves indicates good quality samples, and mobility of order of 1300–1500 $cm^2/V\,s$ were measured by Hall measurements in the Van der Pauw geometry. Some samples, kept at 300 °C, were exposed for 3 min to an atomic hydrogen flux produced by a remote radio-frequency H_2 plasma[18] or for about 1 h to a very low-energy (10–20 eV) ion beam for different doses of impinging H or He ions. X-ray photoelectron spectroscopy, atomic force microscopy, and spectroscopic ellipsometry showed that In clusters form on the sample surface upon the atomic H treatment. Nevertheless XRD pattern indicated that bulk InN was not structurally changed or In enriched by hydrogenation. Before performing any optical characterization, on-surface indium clusters were removed by etching the samples in $HCl:H_2O=1:3$ for 30 min. Photoluminescence was excited by the 515 nm line of an Ar^+ laser and detected by two different systems: a PbS photodiode, cooled at −30 °C and coupled to a 1 m monochromator, or a liquid nitrogen cooled InGaAs photodiode, coupled to a 0.25 m monochromator. PL measurements have been normalized to the system response.

III. RESULTS AND DISCUSSIONS

A. Photoluminescence line shape fitting

Low-temperature ($T=10$ K) PL spectra of D110 InN epilayer are shown in Fig. 1(a) (solid lines) for samples subjected to different postgrowth treatments. From bottom to top: (i) as grown, a. g.; (ii) irradiated by a low-energy He ion beam at dose $d_{He}=3\times10^{15}$ ions cm^{-2}; (iii) exposed for 3 min to a H_2 plasma; and [(iv) and (v)] irradiated by a low-energy H ion beam at $d_H=3\times10^{15}$ and 5×10^{15} ions cm^{-2}, respectively. All PL spectra exhibit a high-energy edge (HEE), whose slope depends on temperature—not shown here—according to a Fermi distribution function, a clear signature of recombination in degenerate semiconductors. For increasing d_H and irrespective of the H irradiation technique, the PL HEE rigidly and progressively blueshifts, the relative intensity of the low-energy side of the PL band increases and broadens, and the overall emission efficiency decreases. In the He irradiated sample, on the contrary, the HEE almost does not shift and the emission efficiency does not vary sizably.

A quantitative estimate of the total electron concentration $n_c=n_d+n_{ph}$ (where n_d and n_{ph} are the carrier concentrations related to donor impurities and photoexcitation, respectively) has been obtained by an analysis of the PL line shape in terms of carrier recombination in heavily doped, degenerate semiconductors with relaxation of the quasimomentum conservation rule.[20] The PL spectrum intensity is then given by

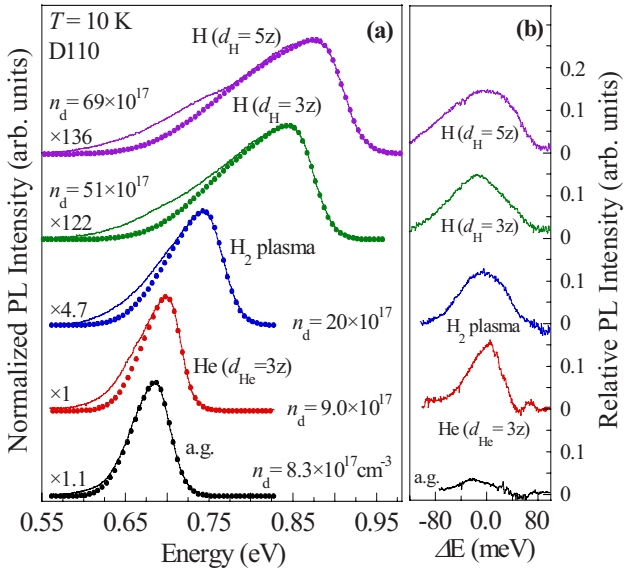

FIG. 1. (Color online) (a) Low-temperature ($T=10$ K) normalized PL spectra (solid lines) of the D110 InN sample for different postgrowth treatments: as-grown (a.g.), hydrogenated for 3 min in a remote H_2 plasma (H_2 plasma), and irradiated at 300 °C with different doses $d_{H,He}$ of low-energy (10–20 eV) H or He ions ($z=1\times10^{15}$ ions cm^{-2}). Normalization factors and carrier concentration related to donors n_d are given in the figure. Laser excitation power density $P_{exc}=200$ W cm^{-2}. Simulations of the PL spectra in terms of the semiclassical model described in the text [see Eqs. (1) and (2)] are given by dots. (b) Difference between the experimental data and simulations (misfit bands) as a function of energy for the same samples shown in panel (a). For each PL spectrum energies are measured with respect to the estimated band gap energy.

$$I(\hbar\omega) \propto \int dE_v \rho_c^{int}(\hbar\omega - E_v)\rho_v(E_v)f_c(\hbar\omega - E_v)f_v(E_v). \quad (1)$$

f_c and f_v are the Fermi quasidistribution functions in the conduction and valence bands, respectively, and $\rho_v(E_v)$ is the three-dimensional density of states (DOS) for the valence band ($\propto\sqrt{E_v}$). $\rho_c^{int}(E)$ is the integrated DOS for the conduction band calculated accordingly to the semiclassical model developed by Kane,[21]

$$\rho_c^{int}(E) = \frac{1}{\pi^2}\int_0^\infty dk_c k_c^2 P\left[E - \left(E_g + \frac{\hbar^2 k_c^2}{2m^*}\right)\right]. \quad (2)$$

$P(E)$ is a Gaussian function whose standard deviation $\sigma = e^2\sqrt{n_d/8\pi\varepsilon^2\kappa}$ depends on the donor impurity concentration n_d and on the inverse Thomas-Fermi screening length $\kappa(n_c)$. E_g is a renormalized band gap energy. The values of the static dielectric constant ($10.5\varepsilon_0$) (Ref. 22) and electron effective mass ($0.07m_0$) (Ref. 23) have been taken equal to those most commonly reported in the literature. The value of n_{ph} was estimated by simulating spectra recorded under different excitation intensities where only the value of n_{ph} was changed. The simulations of Eq. (1) to the data are shown by dots in Fig. 1(a). The calculated line shape is almost insensitive to the choice of the heavy-hole effective mass

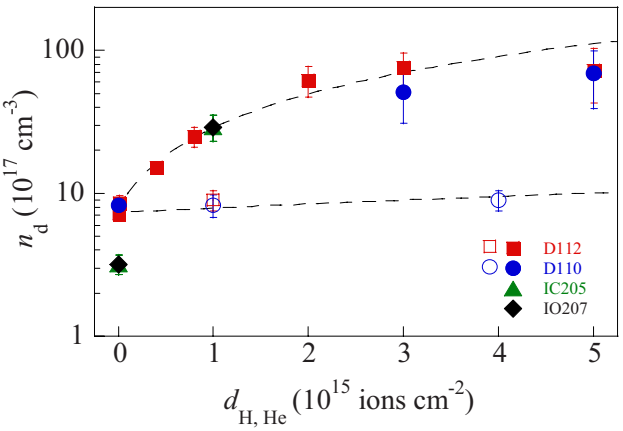

FIG. 2. (Color online) Carrier density related to donors n_d, as estimated from simulations of the PL spectra for differently treated InN samples in terms of the semiclassical model described in the text [see Eqs. (1) and (2)], as a function of implanted dose of hydrogen (full symbols) or helium (open symbols) ions. Dashed lines give linear dependences as a guide to the eyes (notice the different behavior of the H case with respect to the He case).

$(0.2m_0)$.[24] The above semiclassical model reproduces very well all PL band line shapes, but for the low-energy side of each PL band, in terms of three parameters: E_g, n_d, and the carrier temperature T_c. The estimated n_d values, which are substantially unaffected by $\pm 10\%$ changes in the value of the electron effective mass and/or dielectric constant, are shown in Fig. 2 in a semilogaritmic plot for InN samples irradiated with H (full symbols) or with He (open symbols). Consistently with the initial assumption of a degenerate semiconductor, the carrier concentration in the as-grown sample ($n_d = (3-9) \times 10^{17}$ cm^{-3}) is well above the concentration of the insulator-to-metal transition in InN, whose value ranges[12,25] from 0.5×10^{17} to 2×10^{17} cm^{-3}. *Independently of the carrier concentration in the as-grown sample*, n_d increases almost linearly (dashed lines in the figure) with the dose of impinging ions. However, the carrier concentration in the He irradiated sample increases at a rate about 2 orders of magnitude *slower* than in the case of the H irradiated sample. Therefore, most of the donors created by low-energy H irradiation are not due to sample damage, contrary to the case of the donors produced by high-energy (2 MeV) implantation with H^+ or $^4He^+$ ions reported in Ref. 16. Therein, indeed, the increase in carrier concentration achieved by $^4He^+$ ions was approximately three times *higher* than that achieved by a same dose of H^+ ions, as expected in the case of radiation damage.

It has been already pointed out that the semiclassical model reproduces very well all PL band line shapes, but for the low-energy side of each PL band. The difference, or misfit, between experimental data and line shape simulation has been evaluated for each of the PL spectra shown in Fig. 1(a). The resulting misfit bands are shown in Fig. 1(b) as a function of the photon energy ΔE, which has been measured with respect to the band gap energy as obtained from the simulation of each spectrum. These bands have roughly Gaussian line shapes and are centered below the band gap energy. In the as-grown sample, the misfit band is very weak and poorly defined, if ever present, while it increases in relative intensity and broadens for increasing d_H in the three hydrogenated samples. Since the band integrated intensity increases with estimated carrier density n_d, this band is attributed to the (H,h) recombination of an electron bound to a H donor with a free hole in the valence band. By averaging over the values obtained from the PL spectra in all hydrogenated samples, the energy level of the H donor is estimated to be 10 ± 5 meV below the conduction band edge. The uncertainty in the donor binding energy accounts for the changes from one spectrum to the other as well as for small changes in the electron effective mass, or for a small $(\pm 10\%)$ supposed dependence on energy of this mass. It should be noticed that a misfit band is present also in the case of the He irradiated sample. However, the center of mass of this band is very close (−2 meV) to the band gap energy. Therefore, this band has an origin completely different from that induced by H irradiation, as it will be confirmed by thermal annealing experiments. It most likely originates from distorted bonds (Urbach's tail) produced by the $^4He^+$ bombardment.

B. Thermal annealing

Additional information on the donor nature of H in *n*-type InN is gathered by analyzing the changes in the PL line shape upon isothermal or isochronal thermal annealing. The PL spectra of the sample D110, hydrogenated in a H_2 plasma and subjected to different times of isothermal annealing at 325 °C, are shown in Fig. 3 together with their theoretical simulations. A 24 h annealing leads to an almost complete recovery of the line shape of the as-grown sample and to a full recovery of its PL intensity, as shown in the inset.[26] On the one hand, the recovery of the line shape of the as-grown sample upon this *mild* annealing indicates a *highly mobile* nature of the H-related donors. On the other hand, the lack of a full recovery of the as-grown sample PL line shape suggests that H irradiation leads also to the formation of lowly mobile defects with density more than 1 order of magnitude smaller than that related to H donors. These lowly mobile defects are possibly the same defects responsible for native excess electrons in the as-grown sample, namely, N vacancies V_N as thoroughly discussed in Ref. 18. These vacancies, indeed, behave as donors and have the lowest formation energies[17,27] among *native defects* in *n*-type InN.

The values of the carrier concentration as estimated from the simulations are shown in Fig. 4 vs annealing time, t_a, for different annealing temperatures, T_a, of the sample treated in a H_2 plasma (full symbols) and of a He irradiated sample (open symbols). The process of H debonding from a stable site in the host lattice and H diffusion out of the crystal is usually described[28] by the equation

$$n_d = n_H + n_r = n_0 e^{-\nu t_a e^{-E_a/k_B T_a}} + n_r, \tag{3}$$

namely, in terms of a single activation energy E_a for H outdiffusion. n_0 is the initial H-donor concentration after sample hydrogenation, ν is the attempt frequency of H in the equilibrium site, and n_r accounts for a residual concentration of

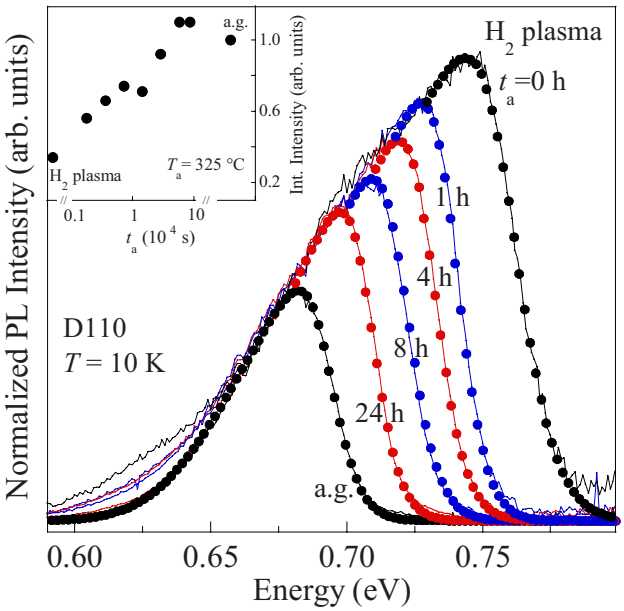

FIG. 3. (Color online) Low-temperature (T=10 K) PL spectra (solid lines) of D110 InN sample submitted to different treatments: as-grown (a.g.), hydrogenated for 3 min in a remote H_2 plasma (H_2 plasma), and annealed at 325 °C for increasing time t_a. Laser excitation power density P_{exc}=20 W cm^{-2}. The spectra have been normalized at 0.67 eV for ease of comparison. Simulations of the PL spectra in terms of the semiclassical model described in the text [see Eqs. (1) and (2)] are given by dots. Inset: PL integrated intensity vs annealing time.

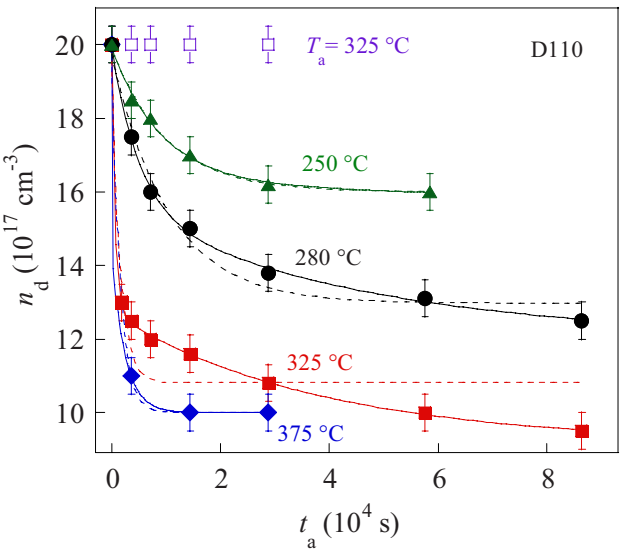

FIG. 4. (Color online) Carrier density related to donors n_d (full symbols) vs annealing time t_a as derived by simulating the PL data taken in sample D110 exposed for 3 min to a H_2 plasma and then annealed at T_a=250 °C (triangles), 280 °C (dots), 325 °C (squares), and 375 °C (diamonds). Fits of Eq. (4) to the data in terms of two H activation energies are shown by solid lines. Dashed lines are fits to the data by using a single activation energy; see Eq. (3). n_d in the sample irradiated with He (d_{He}=1.1 $\times 10^{17}$ ions cm^{-2}) and then annealed at T_a=325 °C is shown as a function of t_a by open squares (notice the different behavior with respect to the H case).

carriers, including those of the as-grown sample, which is not affected by thermal annealing.[26] However, this procedure based on a single activation energy is highly unsatisfactory. First, good fits of Eq. (3) to the isothermal annealing data (dashed lines) cannot be obtained with a same value of E_a for all the four annealing temperatures: E_a increases from 1.88 to 1.99 eV, to 2.05 eV, and finally to 2.23 eV, for temperature increasing, respectively, from 250 to 280 °C, to 325 °C, and to 375 °C. Second, fits of Eq. (3) to the data at the two intermediate temperatures of 280 and 325 °C are quite poor. Third, the good fit achieved at 250 °C indicates that n_d saturates at 16×10^{17} cm^{-3}, a value almost doubled with respect to that estimated in the as-grown sample (8.3×10^{17} cm^{-3}). These three points altogether clearly indicate that a second H-related donor specie, at least, contributes to the carrier concentration in hydrogenated samples.

As a matter of fact, excellent fits (solid lines) have been obtained for *all the four annealing temperatures*[29] by assuming the existence of two stable sites for H in the host lattice and introducing, therefore, two different thermal activation energies for H outdiffusion

$$n_d = n_H + n_r = n_{01}e^{-\nu_1 t_a e^{-E_{a1}/k_B T_a}} + n_{02}e^{-\nu_2 t_a e^{-E_{a2}/k_B T_a}} + n_r, \tag{4}$$

where n_{0i} are the H-donor initial concentrations in the two sites, ν_i and E_{ai} are the corresponding attempt frequencies and activation energies, respectively, and n_r accounts for a residual concentration of carriers, including those of the as-grown sample, which are not affected by the annealing

TABLE I. Values (and standard deviations) of the parameters entering the best fits of Eq. (4) to the annealing data, as obtained from separately averaging the values obtained from the fits of the whole set of isothermal *or* isochronal annealings. Parameter values averaged over the whole set of isothermal *and* isochronal annealings are also shown in the third row. E_{ai} are the activation energies for H debonding, n_{0i} are the carrier concentrations of each H species at the beginning of the annealing, and n_r is the residual carrier concentration after an infinite time of annealing; see Eq. (4).

Annealing	E_{a1} (eV)	n_{01} (10^{17} cm^{-3})	E_{a2} (eV)	n_{02} (10^{17} cm^{-3})	n_r (10^{17} cm^{-3})
Isothermal	2.20 ± 0.06	5.0 ± 1.4	1.95 ± 0.06	5.0 ± 1.6	9.7 ± 0.4
Isochronal	2.17 ± 0.01	3.4 ± 1.2	1.99 ± 0.05	3.7 ± 1.2	10.6 ± 0.4
Average	2.18 ± 0.07	3.8 ± 0.4	1.97 ± 0.06	4.5 ± 0.9	10.2 ± 0.5

process.[18] The values of the best fitting parameters, as obtained from an average of the fits of the *whole set of isothermal annealing data*, and of their standard deviations are shown in the first row of Table I. The values of the attempt frequencies have been kept equal to those estimated for the stretching frequencies of interstitial H^+ in the antibonding nitrogen AB_N site (ν_1=3412 cm^{-1}) and the bond center BC site (ν_2=3069 cm^{-1}). The AB_N and the BC sites have been theoretically predicted[30,31] to be almost equivalent stable sites for H in wurtzite InN.

It should be now clear why annealings at 250 and 375 °C could be fitted reasonably well in terms of a single activation energy, *but with quite different values at the two temperatures*. The concentration of the carriers related to the second H species, whose debonding activation energy is 2.20 eV, decreases by only 0.5% after a 16 h annealing at 250 °C. Therefore, at low annealing temperature this second H species shows up only as an increase in the background concentration, almost twice that in the as-grown sample. For the opposite reason, annealing data at 375 °C could be fitted in terms of a single activation energy 0.25 eV higher than that required to fit the 250 °C annealing data: for an activation energy of 1.95 eV, the carrier concentration decreases to 1% of the initial value after just a 60 s annealing at 375 °C. Therefore, *only at intermediate temperatures* the release of *both species of hydrogen can be followed as a function of annealing time*, and both activation energies are required in Eq. (4) to achieve a good fit of data. Within the experimental uncertainty, these activation energies are the same as those separately required to fit well the data at the lowest (250 °C) and the highest (375 °C) annealing temperatures.

The value of n_r is higher by ~20% than that of n_d in the as-grown sample, thus showing that H irradiation contributes also to a small fraction of highly stable, lowly mobile defects, most likely N vacancies as discussed before. Similar concentrations of lowly mobile defects are produced by irradiating the sample with a dose of He ions (d_{He}=1.1 $\times 10^{17}$ ions cm^{-2}) more than 100 times *higher* than that necessary to obtain the same n_d value by H ion irradiation. The activation energy for the removal of these He-induced donors is much higher than that characterizing H-donor removal, as evidenced by the isothermal annealing data shown in Fig. 4 (open squares). This feature confirms the completely different nature of these He-related donors with respect to H donors.

The existence of at least two different, highly mobile H-related donors is also required in order to fit the peculiar dependence of n_d on T_a as measured for isochronal annealings and shown in Fig. 5. Indeed, 4 and 8 h (as well as 1 h, not shown here) annealing data (symbols) can be fitted well (solid line) only in terms of two activation energies. The slight misfit at T_a=375 °C is due to the beginning of desorption of the third, lowly mobile donor specie discussed before. The values of E_{a1} and E_{a2} well match those found from the isothermal annealings shown in Fig. 4; compare first and second rows in Table I. Similar results have been obtained in H beam irradiated samples where achieved carrier concentrations were even higher, as well as in samples with different substrates.

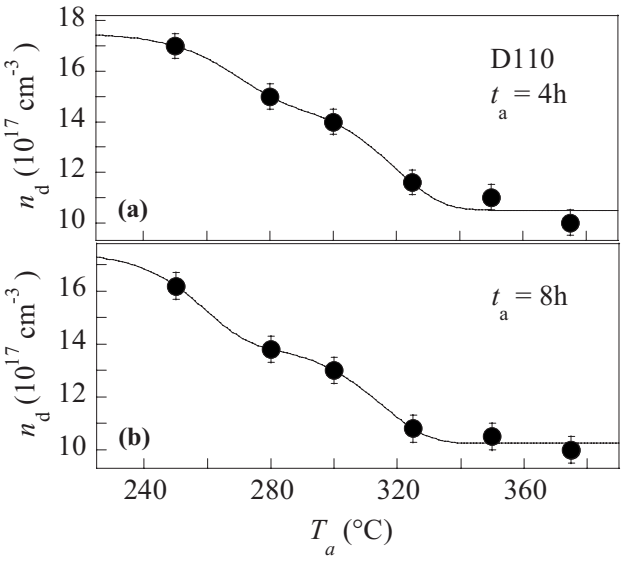

FIG. 5. Carrier density related to donors n_d in the sample D110 is reported as a function of annealing temperature T_a for t_a=4 h in panel (a) and for t_a=8 h in panel (b). Fits of Eq. (4) to the data in terms of two H activation energies are shown by solid lines.

Some hints on the microscopic nature of the two different H equilibrium sites may be provided by calculations based on density functional theory within the local density approximation. These calculations predict that H has two stable equilibrium sites in zinc blende[9,17] and wurtzite[30] InN, the antibonding nitrogen AB_N site and the bond center BC site, where H behaves as a donor, independently of *n*- or *p*-type doping. The AB_N site is slightly more stable than the BC site: the total energy for the AB_N site is 0.18 eV lower than that of the BC site in zinc blende[17] InN (0.15 eV in wurtzite[30] InN). The formation energy of the two sites is almost the same, too. These data are consistent with our experimental findings that, on the average, E_{a1} and E_{a2} differ by only ~0.21 eV and n_{01} and n_{02} are equal within the experimental uncertainty; see third row in Table I. It should be noticed here also that the experimental uncertainty in the activation energies, typical for this type of data analysis,[32] may reflect small differences between the dissociation of H–N bonds parallel or perpendicular to the wurtzite *c* axis as well as the structural disorder of these highly defected samples. Finally, the H species having the higher experimental activation energy should correspond to H in the more stable AB_N site, where its activation energy (~2.18 eV) would be very close to that found in GaAs for AB H-donor complexes having a bond strength similar to that of the N–H bond here discussed.[32]

IV. CONCLUSIONS

In conclusion, photoluminescence measurements demonstrate that H shallow donors (with binding energy equal to about 10 meV) can be produced in *n*-type InN by exposure to a H_2 plasma or to a low-energy H ion beam. Thus, electron concentrations about 2 orders of magnitude higher than

that of the insulator-to-metal transition have been achieved. The decrease in the carrier concentration toward that of the as-grown sample upon different thermal annealing is characterized by two activation energies and provides evidence of different donor species related to H irradiation.

The results presented here emphasize the multiform capability of H to modify dramatically the electronic properties of semiconductors whenever it forms strong bonds with highly electronegative elements such as N and O. As an example, H passivates the effects of isoelectronic doping determined by N in III-V compounds or by O in II-VI compounds.[2–5] Finally, it has been recently debated if H does or does not give rise to a donor state through the formation of multicenter bonds with four Zn atoms in ZnO.[33,34] In this material H acts as a donor also by occupying the AB_O and the BC sites as, *mutatis mutandis*, it does in InN. Therefore, InN appears to be an appropriate test bed for investigating the fascinating properties of H bonds in semiconductors.

ACKNOWLEDGMENTS

The authors acknowledge A. Janotti and C. G. Van de Walle for sharing their theoretical results for H in wurtzite InN, and A. Zunger for useful discussions.

[1] E. Mollwo, Z. Phys. **138**, 478 (1954).
[2] M. Felici, A. Polimeni, G. Salviati, L. Lazzarini, N. Armani, F. Masia, M. Capizzi, F. Martelli, M. Lazzarino, G. Bais, M. Piccin, S. Rubini, and A. Franciosi, Adv. Mater. (Weinheim, Ger.) **18**, 1993 (2006), and references therein.
[3] A. Polimeni, G. Baldassarri H. v., H. M. Bissiri, M. Capizzi, M. Fischer, M. Reinhardt, and A. Forchel, Phys. Rev. B **63**, 201304(R) (2001).
[4] A. Polimeni, M. Bissiri, M. Felici, M. Capizzi, I. A. Buyanova, W. M. Chen, H. P. Xin, and C. W. Tu, Phys. Rev. B **67**, 201303(R) (2003).
[5] M. Felici, A. Polimeni, M. Capizzi, Y. Nabetani, T. Okuno, K. Aoki, T. Kato, T. Matsumoto, and T. Hirai, Appl. Phys. Lett. **88**, 101910 (2006).
[6] C. G. Van de Walle, Phys. Rev. Lett. **85**, 1012 (2000).
[7] C. Kiliç and A. Zunger, Appl. Phys. Lett. **81**, 73 (2002).
[8] C. G. Van de Walle and J. Neugebauer, Nature (London) **423**, 626 (2003).
[9] C. G. Van de Walle and J. Neugebauer, J. Appl. Phys. **95**, 3851 (2004), and references therein.
[10] For a review, see W. Walukiewicz, J. W. Ager III, K. M. Yu, Z. Liliental-Weber, J. Wu, S. X. Li, R. E. Jones, and J. D. Denlinger, J. Phys. D **39**, R83 (2006), and references therein.
[11] V. M. Polyakov and F. Schwierz, Appl. Phys. Lett. **88**, 032101 (2006).
[12] T. Inushima, M. Higashiwaki, T. Matsui, T. Takenobu, and M. Motokawa, Phys. Rev. B **72**, 085210 (2005).
[13] R. E. Jones, K. M. Yu, S. X. Li, W. Walukiewicz, J. W. Ager, E. E. Haller, H. Lu, and W. J. Schaff, Phys. Rev. Lett. **96**, 125505 (2006).
[14] E. A. Davis, S. F. J. Cox, R. L. Lichti, and C. G. Van de Walle, Appl. Phys. Lett. **82**, 592 (2003).
[15] D. C. Look, H. Lu, W. J. Schaff, J. Jasinski, and Z. Liliental-Weber, Appl. Phys. Lett. **80**, 258 (2002).
[16] S. X. Li, K. M. Yu, J. Wu, R. E. Jones, W. Walukiewicz, J. W. Ager, W. Shan, E. E. Haller, Hai Lu, and William J. Schaff, Phys. Rev. B **71**, 161201(R) (2005).
[17] S. Limpijumnong and C. G. Van de Walle, Phys. Status Solidi B **228**, 303 (2001).
[18] Maria Losurdo, Maria M. Giangregorio, Giovanni Bruno, Tong-Ho Kim, Soojeong Choi, April S. Brown, Giorgio Pettinari, Mario Capizzi, and Antonio Polimeni, Appl. Phys. Lett. **91**, 081917 (2007), and references therein.
[19] V. Lebedev, V. Cimalla, J. Pezoldt, M. Himmerlich, S. Krischok, J. A. Schaefer, O. Ambacher, F. M. Morales, J. G. Lozano, and D. González, J. Appl. Phys. **100**, 094902 (2006).
[20] See, e.g., A. R. Goñi and K. Syassen, in *High Pressure in Semiconductor Physics I*, Semiconductors and Semimetals, R. K. Willardson and E. R. Weber Series editions, edited by T. Suski and W. Paul (Academic, San Diego, CA 1998), Vol. 54, p. 324.
[21] E. O. Kane, Phys. Rev. **131**, 79 (1963).
[22] T. Inushima, M. Higashiwaki, and T. Matsui, Phys. Rev. B **68**, 235204 (2003).
[23] J. Wu, W. Walukiewicz, W. Shan, K. M. Yu, J. W. Ager, E. E. Haller, H. Lu, and W. J. Schaff, Phys. Rev. B **66**, 201403(R) (2002).
[24] Y.-N. Xu and W. Y. Ching, Phys. Rev. B **48**, 4335 (1993).
[25] J. S. Thakur, Y. V. Danylyuk, D. Haddad, V. M. Naik, R. Naik, and G. W. Auner, Phys. Rev. B **76**, 035309 (2007).
[26] Notice that the PL spectrum of the as-grown sample does not change upon annealing for 8 h at 300 °C; see Ref. 18.
[27] However, the formation energy of positively charged N vacancies in *n*-type InN has been predicted to be quite high; see Ref. 9. Therefore, kinetic effects should justify the formation out of equilibrium of a sizable concentration of N vacancies. See also C. Stampfl, C. G. Van de Walle, D. Vogel, P. Krüger, and J. Pollmann, Phys. Rev. B **61**, R7846 (2000).
[28] M. Bissiri, G. B. von Högersthal, A. Polimeni, M. Capizzi, D. Gollub, M. Fischer, M. Reinhardt, and A. Forchel, Phys. Rev. B **66**, 033311 (2002).
[29] In the case of the highest temperature (375 °C), the simulation is almost insensitive to the value of the lower activation energy, which has been taken equal to 1.95 eV.
[30] A. Janotti and C. G. Van de Walle (private communication).
[31] The attempt frequency and the activation energy are "entangled" parameters in the fitting procedure. However, changes in the attempt frequencies from 2000 to 4000 cm^{-1} lead to changes of only 1.7% (namely, 31 meV, much less than the reported experimental uncertainty) in the value of the activation energy. On the other hand, carrier densities at the beginning of annealing period (n_{0i}) and attempt frequencies are fully uncorrelated.
[32] S. J. Pearton, W. C. Dautremont-Smith, J. Chevallier, C. W. Tu, and K. D. Cummings, J. Appl. Phys. **59**, 2821 (1986).
[33] A. Janotti and C. G. Van de Walle, Nat. Mater. **6**, 44 (2007).
[34] H. Takenaka and D. J. Singh, Phys. Rev. B **75**, 241102(R) (2007).